

Gradient domain photomontage via interactive object selection

Bekir DİZDAROĞLU*

Department of Computer Engineering, Faculty of Engineering, Karadeniz Technical University, Trabzon, Turkey

Received: 01.12.2014

Accepted/Published Online: 28.08.2015

Final Version: 30.05.2018

Abstract: One of the most critical steps in photomontage is marking an object that is to be copied from a source image to a target image efficiently. Some unexpected and unwanted effects such as bleeding usually occur on the resulting image if the object is roughly marked, copied, and then pasted to the target region, even when using the Poisson equation approach. Moreover, original color information for the pasted object cannot be preserved, and color values for the boundary pixels of the pasted object may change and/or blurriness may occur when using some methods described in the literature. The proposed methods presented in this paper are designed to efficiently overcome these problems. The problem of rough selection is solved by employing the modified intelligent scissors method. In order to prevent diffusion around the boundary of the pasted object, a band region is created, and the texture information from the source image is used. In order to better preserve the color information of the pasted object, a fidelity term is added to the Poisson equation. Our approach for producing a photomontage is more efficient than other methods in the literature in terms of interactive object selection and automated band region creation. In our approach, readjustment is not necessary for required parameters in the operations. Qualitative and quantitative results prove the advantages of the proposed methods.

Key words: Band region, fidelity term, finite differences, gradient vector field, interactive object selection, photomontage, Poisson equation, spectral method

1. Introduction

Photomontage is an image editing operation in which a part of an image (target) is replaced by a part of another image (source) so that the transition in the boundaries of the edited region is hardly noticeable with the naked eye or using a digital apparatus. One basic method for this process is a classical direct copy-paste operation. The most fundamental problem in the direct copy-paste operation is that the boundaries of the edited region can be easily and clearly distinguished with the naked eye. This drawback of the direct copy-paste operation can be eliminated by applying the Poisson equation, which commonly uses partial differential equations (PDEs) [1]. PDEs can be classified into elliptic, parabolic, and hyperbolic equations. The Poisson equation is a linear second-order elliptic PDE and is solved by finite differences [1–4], finite elements [5], or spectral methods [6,7]. Finite differences are employed in many methods because of their simplicity in solving the Poisson equation [8].

The first question to answer in photomontage is: How should a region in the source image be selected? A freehand rough selection approach, such as the Lasso tool in Adobe Photoshop, can be employed to roughly mark the region. Depending on how rough the selection is, some unwanted effects are revealed, i.e. blurring or bleeding can occur near the edited region, and dominant texture information of either the source image or the

*Correspondence: bekir@ktu.edu.tr

target image in the edited region may be mixed with one another. In order to eliminate these drawbacks, the boundary of the object in the source image needs to be determined by employing an interactive segmentation technique due to the fact that automated methods in the literature may not be successful in the segmentation [4]. The graph-cuts-based method [2,9], the random walk method [10], and the geodesic method [11], or the composition of the random walk method and the geodesic method [12], require some strokes from the user to roughly classify the object and the background. These methods generate sufficient or insufficient segmentation results depending on the locations and the numbers of user strokes that provide the region information. Although there is an image matting method [13] that produces an efficient result, the method also depends on user strokes. Another method called Bayesian image matting [14] is used to extract an object from the background based on a mask created by the user. The Magnetic Lasso tool in Adobe Photoshop is another freehand selection method. This method, called intelligent scissors [15], utilizes only the edge information based on some criteria in the edited image and can be employed to properly select the object boundary in the source image.

Another problem in photomontage is the changes in the color information of the object pasted to the target region. In order to avoid this inconvenience, another parameter called the fidelity term is added to the Poisson equation [4].

The Poisson equation utilized in conducting photomontage can be resolved by employing either iterative [1,2] or direct methods [3,4,6,7]. Direct methods can find the solution faster than the iterative methods. Moreover, some methods take the whole image region [3,6] into account, while others only take the edited part of the image into account [1,4] to produce the resulting image. In the former case, the boundary parts of the pasted object may sometimes get blurry, or the change in intensities near the boundary region may reach a level that is high or low enough to be noticed with the naked eye. This problem can be resolved by adding weighting coefficients to the Poisson equation [3]. However, this approach may cause changes in intensities of the background as well. On the other hand, for the latter case in solving the equation, some defects may sometimes occur and these defects can easily be noticed with the naked eye. For instance, the copied object and its boundary region may get darker or brighter.

This study employs the modified intelligent scissors method for selecting the object boundary and proposes some methods of photomontage based on direct and iterative methods using finite differences to solve the Poisson equation.

2. Photomontage

First the symbols used in this study are introduced. As illustrated in Figure 1, $s : \Gamma \rightarrow \mathbb{R}^2$ shows the source image from which the object $g : \Omega_1 \rightarrow \mathbb{R}^2$ is selected, and $h : \Omega_2 \rightarrow \mathbb{R}^2$ shows the band region created around the boundary of the selected object. Let f^* and f respectively be the target image to paste the object and the resulting image defined in the region $\Omega \rightarrow \mathbb{R}^2$. Let $\mathbf{x} = (x, y) \in \Omega$ denote any point in the whole image domain.

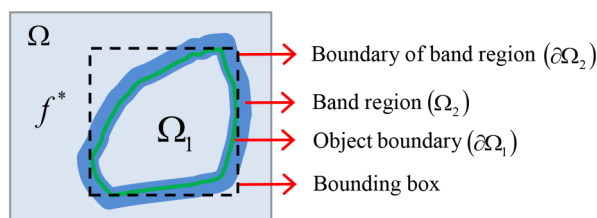


Figure 1. Graphical representation of photomontage for this study.

3. Classical photomontage methods

The Poisson equation for photomontage is given as follows [1]:

$$\min_{f \in \Omega_1} \int_{\Omega_1} |\nabla f - \nabla g|^2 d\mathbf{x}, \text{ with } f|_{\partial\Omega_1} = f^*|_{\partial\Omega_1} . \quad (1)$$

The numerical solution of Eq. (1), depending on the Dirichlet boundary conditions, can be achieved by either direct methods or iterative ones. Iterative methods include the successive over-relaxation (SOR) method [1], while direct ones include the lower-upper factorization (LU) method [4], which is a sparse linear system solution. The following expression can be written for the SOR method:

$$\begin{aligned} f(\mathbf{x})^{(n+1)} &= f(\mathbf{x})^{(n)} + \frac{\alpha}{4} \times \\ &[f(x-1, y)^{(n+1)} + f(x, y-1)^{(n+1)} - 4f(\mathbf{x})^{(n)} + f(x+1, y)^{(n)} + f(x, y+1)^{(n)} - \Delta g(\mathbf{x})], \quad (2) \\ &\text{with } f|_{\partial\Omega_1} = f^*|_{\partial\Omega_1} . \end{aligned}$$

Here, the superscript n shows the iteration count. In this study, considering the SOR method, only a rectangular bounding box with the size of $P \times Q$ pixels, containing the edited region, is taken into account as depicted in Figure 1. Furthermore, α is taken as the smaller positive root of the second-order equation:

$$\left[\cos\left(\frac{\pi}{P}\right) + \cos\left(\frac{\pi}{Q}\right) \right]^2 \alpha^2 - 16\alpha + 16 = 0. \quad (3)$$

Initialization values of unknown pixels in the region Ω_1 are set using g . The iteration is terminated based on Eq. (4):

$$\left\| f^{(n+1)} - f^{(n)} \right\|_{L^\infty} \equiv \max_{\mathbf{x} \in \Omega_1} \left| f^{(n+1)}(\mathbf{x}) - f^{(n)}(\mathbf{x}) \right| \leq \varepsilon. \quad (4)$$

Here, a small ε is chosen as a threshold value.

Although the SOR and LU methods generate almost the same results, the LU method arrives at the solution faster. In the SOR method [1] and LU method [4], the edited region Ω_1 and its roughly selected surrounding region are considered.

There are other methods in which the whole image region Ω is considered. One of them, a direct spectral method [6], uses the discrete Fourier transform (DFT). With the DFT, the Poisson equation can be directly solved based on Neumann boundary conditions.

4. Interactive image segmentation methods

Some blurring occurs on the resulting image if the object is selected from the source image using the Lasso tool and if the region on the target image where the selected object is pasted contains dominant data such as texture. In order to eliminate this problem, a method based on the maximum gradient data of the source and target regions was presented in [1]. However, this method does not give satisfactory results if not only the target image but also the source image contains dominant texture data. For this reason, the boundary of the object should be determined a priori using an interactive segmentation method before editing. In the graph-cuts methods [2,9], the user initially marks some pixels in the interior and exterior parts of the object. These marked pixels are called hard constraints that contain approximate region information about the object and the background. These pixels are also used as seed points in the segmentation process. These methods use boundary information based on created graph nodes that represent pixels and graph edges containing gradient

information of the neighboring pixels related to the processing pixels as well. If the segmentation result is insufficient, the user marks some additional pixels as seed points or removes some marked pixels, and then the segmentation process is repeated. It is pointed out that the method reasonably depends on the number of seed points [12]. In the composition of the random walk method and the geodesic method [12], the user has to mark some pixels as seed points to start the segmentation process, although the method is less dependent on the locations and the number of seed points when compared to the graph-cuts method, the random walk method, and the geodesic method. In the image matting method [13], the segmentation results are sufficient for images having especially fine details such as hair. However, the method is also tender on well-marked seed points to extract any object from the image and readjusting all parameters for different objects. Lastly, another Bayesian image matting method [14] tries to extract an object from the background via a user-aided three-level mask (inner, outer, and transition regions). However, in most cases, backgrounds in the edited images have simple structures such as almost flat regions. Moreover, such a method generates the result very slowly and is not very preferable in terms of performance. As seen in Figures 2a–2h, the composition method generates a proper segmentation result compared to others (note that default parameters are used for the implementation of the methods). However, the composition method reveals rounding effects in the object boundaries containing fine details as depicted in Figures 2c and 2d (enclosed with red rectangles). For this reason, we prefer a freehand selection method in this study. Freehand rough object selection presented in [4] is sometimes not efficient for object segmentation due to the fact that the object and the background have almost the same structures or texture information. In conclusion, another freehand selection approach called the intelligent scissors method [15] is more suitable for photomontage.

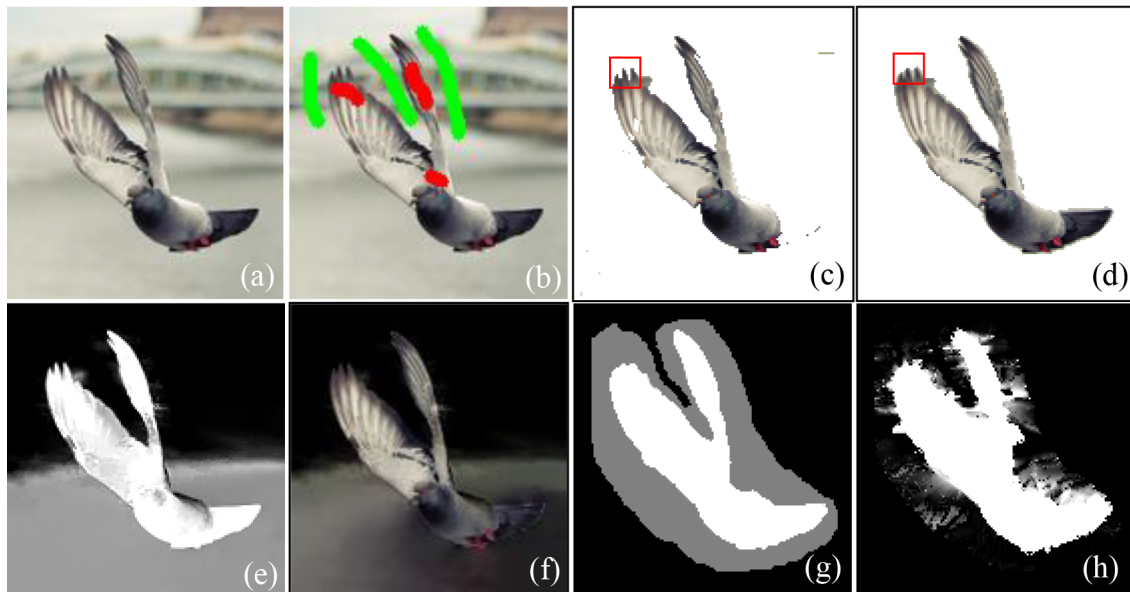


Figure 2. Interactive image segmentation: a) source image with the size of 139×146 pixels, b) marked pixels in the object and background regions, c) segmentation result of the graph-cut method [9], d) segmentation result of the composition of random walk method and geodesic method [12], e) generated mask image of the image matting method [13], f) object extraction result of the image matting method [13], g) user-aided three-level mask for the Bayesian image matting method [14], h) generated alpha-matte mask of the Bayesian image matting method [14].

5. Proposed methods

The biggest problem in state-of-the-art photomontage is that the full extraction of the object in the source image can only be possible with many inputs provided by users. In our approach, in order to overcome such a problem, we first use a modified semiautomated object selection method, where the parameters are not to be continually reset for different objects when the user switches among different objects. Secondly, we employ an automatically created band region to conceal some artifacts in the resulting image. As a result of these operations, we aim to minimize the dependency on the parameters. More detailed information is given in the subsections related to the subject.

6. Modified intelligent scissors method

A modified version of the intelligent scissors method is employed in this study, although it may be slightly slower and more tedious than rough selections. (The same problem occurs in an interactive segmentation method using user strokes. For instance, the user has to carefully draw some strokes without intersection on proper locations of object and background regions.) It is a graph search approach, which is similar to the shortest (minimal cost) path search algorithm [15]. One downside of the intelligent scissors method compared to the freehand rough selection is that the initial contour should be traced more carefully near the boundary, and the boundary is calculated using this method. In the intelligent scissors method [15], the selection of an object based on a local cost function is conducted by tracing the boundaries of the object, weighting the boundary information using Laplacian zero-crossing, magnitude of normalized gradient, and direction of normalized gradient. The local cost function $l(\mathbf{x}, \mathbf{y})$, where \mathbf{x} depicts the location of the processing pixel and $\mathbf{y} = (x, y)$ depicts the location of the neighbors of the processing pixel, is calculated as follows:

$$l(\mathbf{x}, \mathbf{y}) = w_Z s_Z(\mathbf{y}) + w_G s_G(\mathbf{y}) + w_D s_D(\mathbf{x}, \mathbf{y}).$$

Here, w_Z , w_G , and w_D are weights for Laplacian zero-crossing, magnitude of normalized gradient, and direction of normalized gradient. Calculations are given below.

$$s_Z = \begin{cases} 0, & \text{if } \Delta G_\sigma * s = 0 \\ 1, & \text{otherwise} \end{cases}, \tag{5}$$

$$s_G(\mathbf{y}) = 1 - \frac{|\nabla s(\mathbf{y})|}{\max_{\mathbf{y} \in \Gamma} |\nabla s(\mathbf{y})|}, \tag{6}$$

$$s_D(\mathbf{x}, \mathbf{y}) = \frac{2}{3\pi} [\arccos(d_{\mathbf{x}}(\mathbf{x}, \mathbf{y})) + \arccos(d_{\mathbf{y}}(\mathbf{x}, \mathbf{y}))], \tag{7}$$

$$d_{\mathbf{x}}(\mathbf{x}, \mathbf{y}) = \frac{\nabla^\perp s(\mathbf{x})^T}{|\nabla^\perp s(\mathbf{x})|} \ell(\mathbf{x}, \mathbf{y}), \tag{8}$$

$$d_{\mathbf{y}}(\mathbf{x}, \mathbf{y}) = \frac{\nabla^\perp s(\mathbf{y})^T}{|\nabla^\perp s(\mathbf{y})|} \ell(\mathbf{x}, \mathbf{y}), \tag{9}$$

$$\ell(\mathbf{x}, \mathbf{y}) = \begin{cases} \frac{\mathbf{y}-\mathbf{x}}{|\mathbf{y}-\mathbf{x}|}, & \text{if } \frac{\nabla^\perp s(\mathbf{x})}{|\nabla^\perp s(\mathbf{x})|} \left(\frac{\mathbf{y}-\mathbf{x}}{|\mathbf{y}-\mathbf{x}|} \right)^T \geq 0 \\ \frac{\mathbf{x}-\mathbf{y}}{|\mathbf{x}-\mathbf{y}|}, & \text{otherwise} \end{cases}. \tag{10}$$

Here, G_σ is a Gaussian filter with a standard deviation of σ , and $*$ stands for the convolution operator.

In our approach, the binary boundary information is found not only by the Laplacian zero-crossing approach but also by the Canny algorithm (CA) [16], denoted by $s_{CA}(\cdot)$. The CA generates good edge detection results, but the boundaries do not need to be closed, as opposed to the Laplacian zero-crossing approach. Furthermore, by using the CA, fewer false edges are produced, as seen in Figures 3a and 3b. The modified local cost function $l(\mathbf{x}, \mathbf{y})$ is calculated as follows:

$$l(\mathbf{x}, \mathbf{y}) = w_{ZSZ}(\mathbf{y}) + w_{CASCA}(\mathbf{y}) + w_{GSG}(\mathbf{y}) + w_{DSD}(\mathbf{x}, \mathbf{y}). \quad (11)$$

Moreover, in order to mark the boundary of the object in a better way, the size of the source image is scaled to double as shown in Figure 3c.

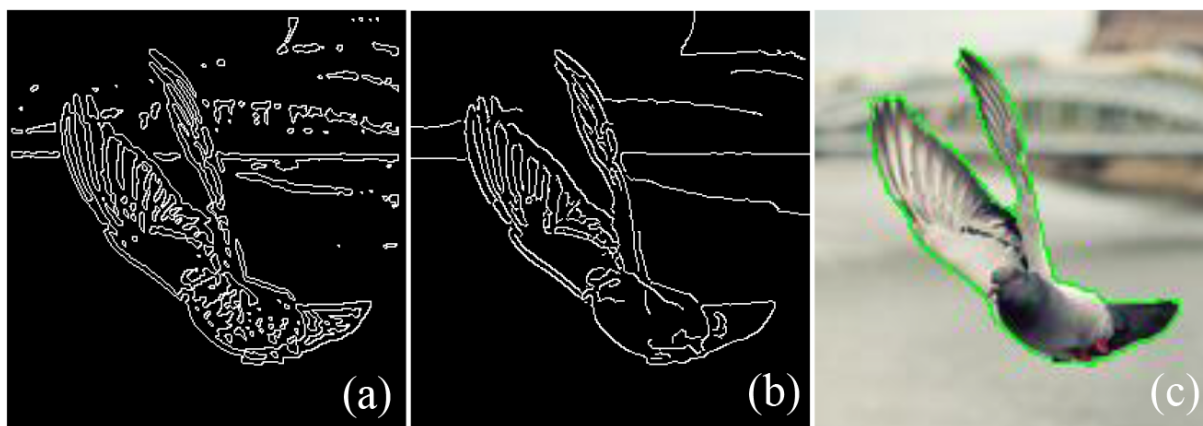


Figure 3. Edge detection and object boundary selection: a) result of the Laplacian zero-crossing method, b) result of the CA method [16], c) object boundary selection with the modified intelligent scissors method.

7. Improved LU and SOR methods

Even if the boundary of the object is selected properly, the color information of the pasted object may not be completely preserved using, for instance, the modified intelligent scissors method in photomontage. In order to better preserve the original color information of the pasted object, a fidelity term [4] should be added to the Poisson equation as indicated in Eq. (12):

$$\min_{f \in \Omega_1} \int_{\Omega_1} |\nabla f - \nabla g|^2 d\mathbf{x} + \lambda \int_{\Omega_1} (f - g)^2 d\mathbf{x}, \text{ with } f|_{\partial\Omega_1} = f^*|_{\partial\Omega_1}. \quad (12)$$

If Eq. (12) is solved based on the Euler-Lagrange method, the statement

$$\lambda f - \Delta f = \lambda g - \Delta g, \text{ with } f|_{\partial\Omega_1} = f^*|_{\partial\Omega_1} \quad (13)$$

is obtained. Thus, Eq. (2) based on the SOR method is revised as:

$$f(\mathbf{x})^{(n+1)} = f(\mathbf{x})^{(n+1)} + \lambda g(\mathbf{x}) - \lambda f(\mathbf{x})^{(n+1)}. \quad (14)$$

Here, λ is a fidelity coefficient that makes an adjustment to preserve the original color of the pasted object to the target image.

The resulting images generated using the SOR and LU methods are quite similar. However, they are different since the estimated values are updated during each iteration, and the iteration is immediately stopped based on a small threshold value in the SOR method. Some problems may occur in both methods. Darkening or brightening may sometimes occur on boundary pixel values of the edited region in the resulting image because some assignments are done from the background to the boundary pixel values of the edited region. In our approach, in order to avoid such problems of boundary pixels encountered with the SOR and LU methods, an automated band region around the object boundary is created, and the texture information on that region is extracted from the source image. These are utilized in eliminating the diffusion as shown below:

$$\min_{f \in \Omega_1 \cup \Omega_2} \int_{\Omega_1 \setminus (\Omega_1 \cap \Omega_2)} |\nabla f - \nabla g|^2 d\mathbf{x} + \int_{\Omega_2} |\nabla f - [(1 - \omega) \nabla f^* + \omega \nabla h]|^2 d\mathbf{x} + \lambda \int_{\Omega_1} (f - g)^2 d\mathbf{x}, \quad (15)$$

with $f|_{\partial\Omega_2} = f^*|_{\partial\Omega_2}$

Here, the weight

$$\omega = 1 - \beta \min \left(1, r(t) \frac{|\nabla h|}{|G_\sigma * \nabla h|} \right) \quad (16)$$

gives texture information in the band region of the source image [3]. Assuming the maximum possible intensity value is 255, $r(t)$ is a function defined as follows [3]:

$$r(t) = \begin{cases} 0, & \text{if } t \leq \eta \\ 1, & \text{if } t \geq 2\eta \\ \frac{t}{\eta} - 1, & \text{otherwise} \end{cases} \quad (17)$$

Here, t is a parameter that is related to the magnitude of the normalized gradient $|\nabla h|$. The band region is generated by morphological operations with a structuring element, unlike the user-aided mask employed in the image matting approach proposed in [14].

8. Spectral method with a fidelity term

In our approach, Eq. (13) is also solved by the DFT based on the Dirichlet boundary conditions in the whole image region Ω unlike the method, which does not include a fidelity term, presented in [6]. Let f_0 be the image generated after the selected region from the source image s is immediately pasted to the target image f^* (direct copy-paste), except for the boundary pixel values of f^* . Let Δf_0 be the Laplacian of f_0 and $M \times N$ be the dimensions of f_0 . f_0 is rearranged as follows.

$$f_0 = \{ 0, f_0(0,0), f_0(1,0), \dots, f_0(M-1, N-1), 0, -f_0(M-1, N-1), -f_0(M-2, N-1), \dots, -f_0(0,0) \}$$

Here, the new dimension of f_0 is extended to $2M \times N + 2$ (note that the new dimension is 4 times the size of the target image in the method presented in [6]). The DFT of f_0 is calculated as:

$$F_0(x) = \left(\frac{i}{2} \mathfrak{S}(f_0) \right) (x+1) \text{ for } x = 0, 1, \dots, (M-1) \times (N-1). \quad (18)$$

Here, $\mathfrak{S}(\cdot)$ indicates the DFT operator and $i = \sqrt{-1}$. The same process is applied to Δf_0 . The solution

of Eq. (13) using the DFT is then reached as indicated below:

$$F(x + y \times M) = \frac{\lambda F_0(x + y \times M) - F_0^\Delta(x + y \times M)}{\lambda - 2 \left[\cos\left(\frac{\pi(x+1)}{M+1}\right) + \cos\left(\frac{\pi(y+1)}{N+1}\right) - 2 \right]} \text{ for } x = 0, 1, \dots, M - 1 \text{ and } y = 0, 1, \dots, N - 1. \quad (19)$$

Here, F , F_0 , and F_0^Δ indicate the rearranged DFT of f , f_0 , and Δf_0 , respectively. Note that after the inverse DFT of F , $f = \frac{4}{(M+1) \times (N+1)} \mathfrak{S}^{-1}(F)$ is calculated, and the boundary pixel values of f^* are directly copied to the extended boundary pixel values of the resulting image f , where the new dimensions are $(M + 2) \times (N + 2)$.

In the DFT approach, some differentiations of the pixel values may occur on the boundary transition of the pasted object. Additionally, blurring may sometimes occur on pixels located on object boundaries. These kinds of problems encountered with whole domain approaches may be eliminated via weighting coefficients [3]. However, in that case, other known pixel values, such as the background pixel values, may change significantly.

9. Experimental results

We tested the performance of the proposed methods on some input images courtesy of Hilal Sönmez and Erkan Barin depicted in Figures 4 and 5 (note that the only reason for the reduction in size of the images is that the resulting images are to be shown in a more efficient manner). The parameters employed in this study are experimentally set. Note that the values of some parameters are borrowed from existing methods in the literature and in most cases small changes in the values of the parameters do not have a negative effect on the generated results. The threshold value ε and the maximum iteration count are set to 0.001 and 250, respectively. The Laplacian of Gaussian filter G_σ with a standard deviation of $\sigma = 1.4$ and a mask size = 9×9 are used for zero-crossing of edges. The weights of the CA and the Laplacian zero-crossing approach are given as $w_{CA} = 0.29$ and $w_Z = 0.14$, respectively. The weight of the coefficient related to the direction of the normalized gradient is kept as $w_D = 0.43$, along with the weight of the coefficient of normalized gradient magnitude, which is kept as $w_G = 0.14$ [15]. λ, β , and η are set to 0.03, 0.99 [3], and 5.1 [3], respectively. In Eq. (16), G_σ is a Gaussian filter with a standard deviation of $\sigma = 0.5$ and mask size = 7×7 [3]. A morphological dilation operator with the

structuring element of $B = \begin{bmatrix} 1 & 1 & 1 \\ 1 & 1 & 1 \\ 1 & 1 & 1 \end{bmatrix}$ is applied to the selected object region. Meanwhile, the morphological

erosion operator with the structuring element of $B = \begin{bmatrix} 1 & 1 \\ 1 & 1 \end{bmatrix}$ is applied separately, and then a band region is obtained by subtracting these from each other.

First we tested the proposed methods for an efficient photomontage. The source and target images are given in Figures 4a and 4b, respectively. The object is selected using the modified intelligent scissors method as depicted in Figure 4c. Figure 4d shows the band region, in which diffusion is avoided by considering the texture information of the pasted object as depicted in Figures 4e and 4f. In Figure 4g, the boundaries of the pasted object can be easily noticed with the naked eye. It should be stated that this object is pasted on the target image using the direct copy-paste method. Some artificial defects occur as seen in Figure 4h when the LU method is directly applied without a fidelity term. This inconvenience stems from the fact that the pixels copied to the boundaries of the edited image region in the target image get darker, depending on the diffusion and the pixels in the other sections of the region. Figure 4i shows the result of the proposed DFT-based method

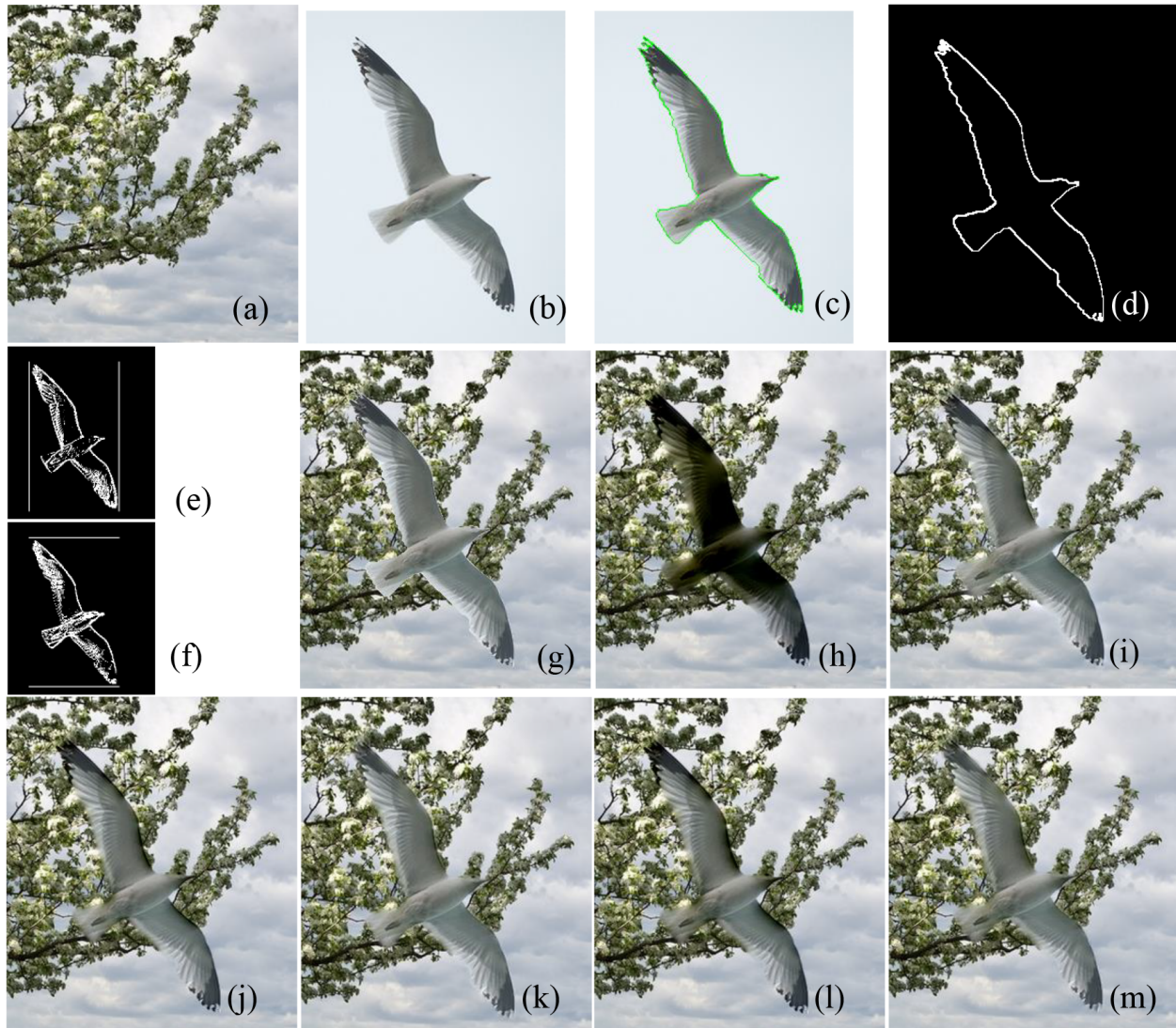


Figure 4. Proposed photomontage methods: a) target image with the size of 285×331 pixels, b) source image with the size of 257×330 pixels, c) selected object from the source image, d) band region, e) texture information obtained from horizontal position, f) texture information obtained from vertical position, g) transferring the selected object to the target image by a direct copy-paste approach, h) proposed Poisson equation method without fidelity term, i) proposed DFT-based method with fidelity term, j) proposed SOR method with fidelity term, k) proposed SOR method with fidelity term-containing band region, l) proposed LU method with fidelity term, m) proposed LU method with fidelity term-containing band region.

where pixel values in the transition region are brighter. In other words, the values of the original pixels of the background image on this transition region could not be preserved. The peak value of signal to noise ratio (PSNR) obtained from the target and resulting images indicating the level of change in values of pixels outside of the edited image region is 30.53 dB for the proposed DFT-based method. In the proposed SOR and LU methods, with the fidelity term-containing band region, darkening did not occur on the pixels of the object boundaries in the generated images (shown in Figures 4j–4m).

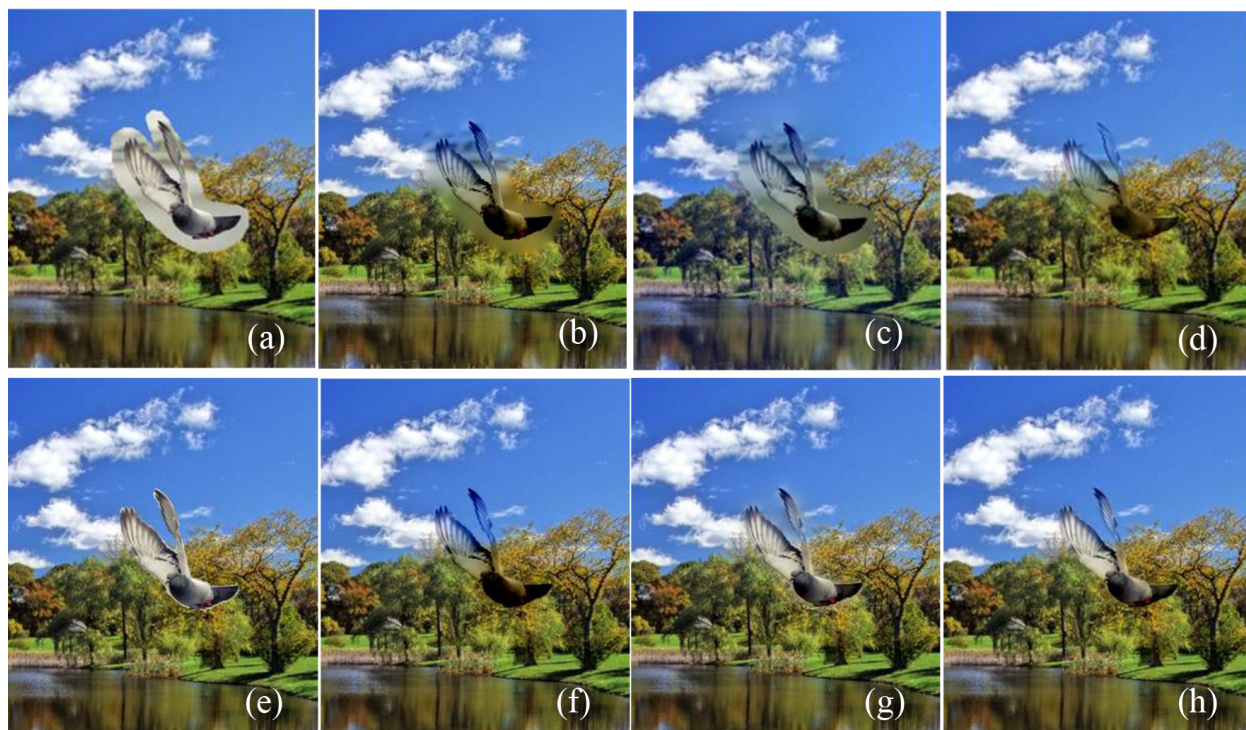


Figure 5. Comparison of photomontage methods: a) transferring the roughly selected object to the target image with the size of 283×330 pixels using direct copy-paste method, b) method presented in [1], c) method presented in [3], d) method presented in [4], e) transferring the selected object to the target region using direct copy-paste method, f) proposed Poisson equation method without fidelity term, g) proposed DFT-based method with fidelity term, h) proposed LU method with fidelity term containing band region.

Some of the existing methods [1,3,4] are also compared with the proposed methods. As illustrated in Figures 5a and 5b, when the object to be pasted is selected roughly but not exactly, some blurring occurs on the resulting image using the method presented in [1]. In that study, the color values of the pasted object could not be preserved and the photomontage could also be easily noticed with the naked eye. The blurring of the image region, edited by the method explained in [3], is avoided, but the values of the known background pixels are also changed (see Figure 5c). Since the object could not be exactly segmented using the method proposed in [4], an acceptable resulting image could not be generated as depicted in Figure 5d. Although the object is selected by the modified intelligent scissors approach (see Figure 5e), a darkened resulting image is generated based on the classical method as depicted in Figure 5f. Even though the DFT-based method is improved by the author, the resulting image is still a little bit brighter, and there is still some blurring (see Figure 5g). The proposed LU method with the fidelity term-containing band region produces the best image among the generated results (see Figure 5h).

The Microsoft Visual C++ platform is used for implementation of the proposed methods. The resulting images depicted in Figures 4i, 4k, and 4m are generated using the proposed DFT-based method with the fidelity term in 6.1 s, using the proposed SOR method with a fidelity term-containing band region in 42.9 s in 106 iterations, and using the proposed LU method with a fidelity term containing-band region in 2.7 s, respectively. The developed code was built and run on a PC with an Intel Core i5-3470 3.20 GHz CPU and with 8 GB of RAM.

10. Conclusion

In this study we present improved methods of photomontage. With the existing methods, different objects are segmented mostly depending on readjustment of parameters and those methods are not always successful in segmentation of the different objects. In our approach, however, the selection of the object is interactively done by the modified intelligent scissors method. Therefore, in most cases, different objects can be successfully edited without depending on readjustment of parameters. Moreover, a fidelity term is added to the direct spectral method depending on the DFT, and a band region is also added to the LU and SOR methods in addition to the fidelity term. Therefore, the color information of the object to be pasted is preserved without bleeding, overbrightening, or overdarkening.

In future studies, the interaction of the color channels in the solution of the proposed equations for multivalued images may be explored in further detail.

References

- [1] Perez P, Gangnet M, Blake A. Poisson image editing. *ACM T Graphic* 2003; 22: 313-318.
- [2] Jia J, Sun J, Tang CK, Shum HY. Drag-and-drop pasting. *ACM T Graphic* 2006; 20: 631-637.
- [3] Tao MW, Johnson MK, Paris S. Error-tolerant image compositing. *Int J Comput Vision* 2013; 103: 178-189.
- [4] Yang W, Zheng J, Cai J, Rahardja S, Chen CW. Natural and seamless image composition with color control. *IEEE T Image Process* 2009; 18: 2584-2592.
- [5] Cuadros VA, Nonato LG, Pascucci V. Combinatorial Laplacian image cloning. In: *The 24th SIBGRAPI Conference on Graphics, Patterns, and Images Tutorials*; 28–30 August 2011; Maceio, Brazil. Danvers, MA, USA: IEEE. pp. 236-241.
- [6] Morel JM, Petro AB, Sbert C. Fourier implementation of Poisson image editing. *Pattern Recogn Lett* 2012; 33: 342-348.
- [7] Bhat P, Curless B, Cohen M, Zitnick CL. Fourier analysis of the 2D screened Poisson equation for gradient domain problems. In: *The 10th European Conference on Computer Vision*; 12–18 October 2008; Marseille, France. Berlin, Germany: Springer. pp. 114-128.
- [8] Iserles A. *A First Course in the Numerical Analysis of Differential Equations*. 2nd ed. New York, NY, USA: Cambridge University Press, 2009.
- [9] Boykov Y, Jolly MP. Interactive graph cuts for optimal boundary & region segmentation of objects in N-D images. In: *The 8th IEEE International Conference on Computer Vision*; July 2001; Vancouver, Canada. Danvers, MA, USA: IEEE. pp. 105-112.
- [10] Grady L. Random walks for image segmentation. *IEEE T Pattern Anal* 2006; 28: 1768-1783.
- [11] Criminisi A, Sharp T, Blake A. GeoS: Geodesic image segmentation. In: *The 10th European Conference on Computer Vision*; 12–18 October 2008; Marseille, France. Berlin, Germany: Springer. pp. 99-112.
- [12] Nguyen TNA, Cai J, Zhang J, Zheng J. Robust interactive image segmentation using convex active contours. *IEEE T Image Process* 2012; 21: 3734-3742.
- [13] Levin A, Lischinski D, Weiss Y. A closed-form solution to natural image matting. *IEEE T Pattern Anal* 2008; 30: 228-242.
- [14] Chuang YY, Curless B, Salesin DH, Szeliski R. A Bayesian approach to digital matting. In: *2001 IEEE Computer Society Conference*; 8–14 December 2001; Kauai, HI, USA. Los Alamitos, CA, USA: IEEE. pp. 264-271.
- [15] Mortensen EN, Barrett WA. Intelligent scissors for image composition. In: *The 22nd Annual Conference on Computer Graphics and Interactive Techniques*; 1995. New York, NY, USA: ACM. pp. 191-198.
- [16] Canny J. A computational approach to edge detection. *IEEE T Pattern Anal* 1986; 8: 679-698.